

Statistical Approach to Nuclear Level Density

R. A. Sen'kov*, V. G. Zelevinsky† and M. Horoi*

*Department of Physics, Central Michigan University, Mount Pleasant, MI 48859, USA

†Department of Physics and Astronomy and National Superconducting Cyclotron Laboratory, Michigan State University, East Lansing, MI 48824-1321, USA

Abstract. We discuss the level density in a finite many-body system with strong interaction between the constituents. Our primary object of applications is the atomic nucleus but the same techniques can be applied to other mesoscopic systems. We calculate and compare nuclear level densities for given quantum numbers obtained by different methods, such as nuclear shell model (the most successful microscopic approach), our main instrument - moments method (statistical approach), and Fermi-gas model; the calculation with the moments method can use any shell-model Hamiltonian excluding the spurious states of the center-of-mass motion. Our goal is to investigate statistical properties of nuclear level density, define its phenomenological parameters, and offer an affordable and reliable way of calculation.

Keywords: Nuclear level density, Fermi-gas model, parity, spin

PACS: 21.10.Ma, 21.10.Dr, 21.10.Hw, 21.60.Cs

MOMENTS METHOD

To describe level densities of a nuclear system in the moments method [1, 2] one needs to introduce a restricted single-particle model space with an effective interaction, as it is usually done in the shell model,

$$H = \varepsilon + V, \quad (1)$$

where ε and V are the one- and two-body parts of the Hamiltonian, correspondingly. The many-body Hilbert space of the problem is divided into partitions κ that are fixed by the occupation numbers of each single-particle orbit. For example, for the case of ^{28}Si in the sd model space there are six valence protons and six valence neutrons to be distributed over the three single-particle orbits, $d_{5/2}$, $s_{1/2}$, and $d_{3/2}$. There are 15 proton and 15 neutron partitions (i.e. 15 different ways of distributing six particles over three sd orbits), which results in total 225 partitions. Each partition can be divided further into smaller subspaces corresponding to exact quantum numbers, such as total spin and parity, $\alpha = J^\pi$.

Let us consider the nuclear level density (NLD) for a given partition κ and a set of quantum numbers α . Such a partial NLD is not well defined, it explicitly depends on the choice of a single-particle basis (the partition κ is not a good quantum number). However, it is known that this partial NLD in the original harmonic-oscillator basis is close to a Gaussian [3], so that the total NLD can be presented as a sum over all the partitions,

$$\rho(E; \alpha) = \sum_{\kappa} D_{\kappa\alpha} G_{\kappa\alpha}(E), \quad (2)$$

where $G_{\kappa\alpha}(E)$ is a finite range Gaussian, $D_{\kappa\alpha}$ is the normalization factor corresponding to the total number of many-body states constructed within a given partition κ for quantum numbers α , and E is the excitation energy. To calculate the finite range Gauss distributions $G_{\kappa\alpha}$ one needs to find the position of each Gaussian (centroid or the first moment), the width (the second moment), and the ground state energy (for more details see, for example, [4, 5], where also the algorithm was presented for subtracting spurious states related to the motion of the nucleus as a whole).

For each configuration ($\kappa\alpha$) we define the first and the second moments of the Hamiltonian (1) as

$$E_{\kappa\alpha} = \langle H \rangle_{\kappa\alpha} \quad \text{and} \quad \sigma_{\kappa\alpha}^2 = \langle H^2 \rangle_{\kappa\alpha} - \langle H \rangle_{\kappa\alpha}^2. \quad (3)$$

Here the average of an operator O is defined as a normalized sum of all diagonal matrix elements calculated within the given configuration,

$$\langle O \rangle_{\kappa\alpha} = \frac{1}{D_{\kappa\alpha}} \text{Tr}^{(\kappa\alpha)} [O] = \frac{1}{D_{\kappa\alpha}} \sum_{n \in (\kappa\alpha)} \langle n | O | n \rangle. \quad (4)$$

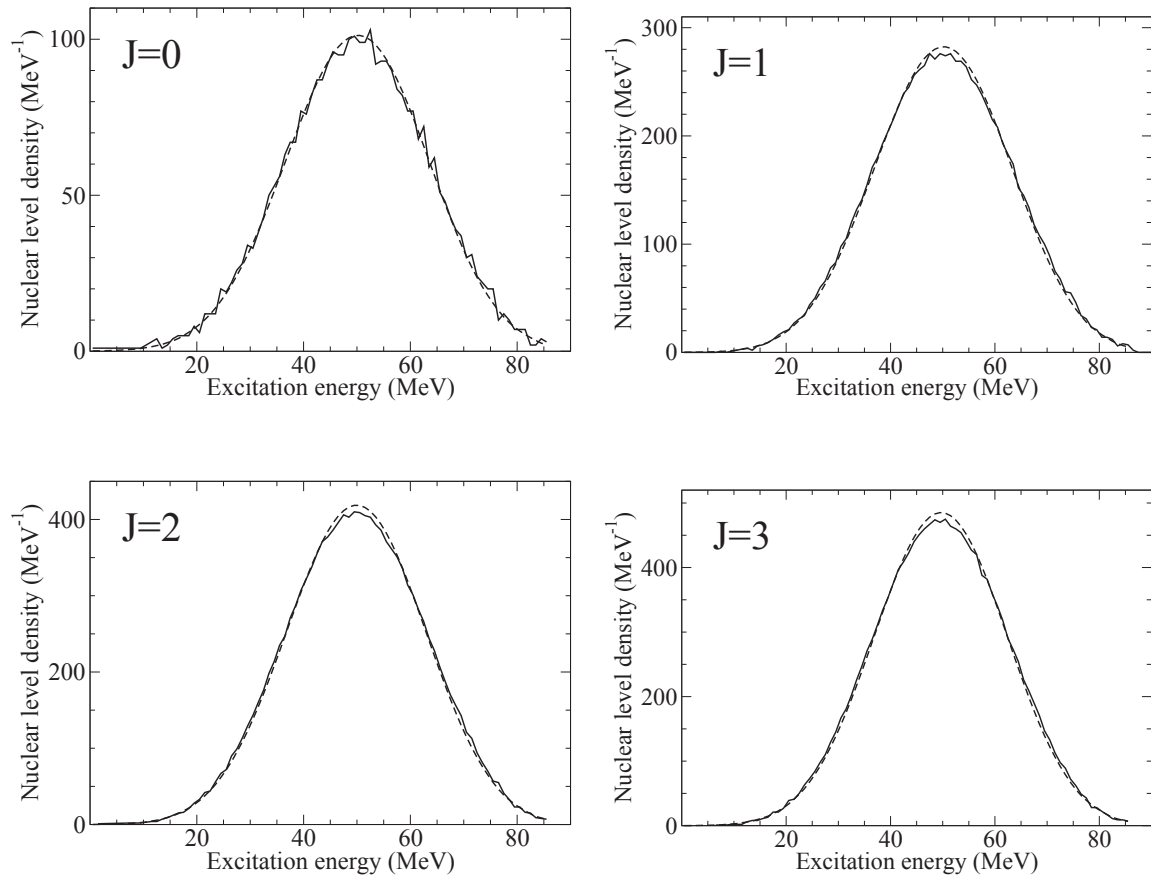


FIGURE 1. Comparison of the shell-model NLD (solid curves) with the moments method densities (dashed curves) calculated for ^{28}Si , sd model space, $J=0, 1, 2$, and 3 , positive parity. USD effective interaction was used [9].

The interaction term in the Hamiltonian (1) fully accounts for the off-diagonal elements between the partitions. The details of calculation of the traces (3) and (4), explanation of the computational algorithm, and the code itself can be found in Ref. [5]. The last ingredient needed for the NLD calculation is the ground state energy that cannot be determined within the moments method. The ground state energy can be obtained using the standard shell model approach for the same model space and the same effective interaction [6] or, for example, using the exponential convergence method [7, 8].

RESULTS

Fig. 1 provides an excellent illustration to the moments method. It presents the comparison of the NLD for the ^{28}Si calculated within the full shell-model diagonalization machinery (solid curves) and by the moments method (dashed curves). Both calculations were performed in the same sd model space and with the same USD effective interaction [9]. Different panels show the NLD corresponding to different spins, $J=0, 1, 2$, and 3 ; all of them demonstrate perfect agreement between the shell model and moments method. The agreement confirms the ideas of quantum chaos and complexity of the majority of states in a closed mesoscopic system of strongly interacting particles put in the foundation of the statistical approach [3, 10]. Fig. 2 compares the NLD of ^{28}Si calculated within the moments method (straight curves) to the experimental level densities (stair curves). There are two stair-case lines on each figure: the solid stair lines present an "optimistic" approach, when all experimental levels with uncertain parity are counted; oppositely, the dashed stair lines present a "pessimistic" approach, when only the experimental levels with assigned parity are included. Again, one can see a fairly good agreement between the densities, of course limited by the space

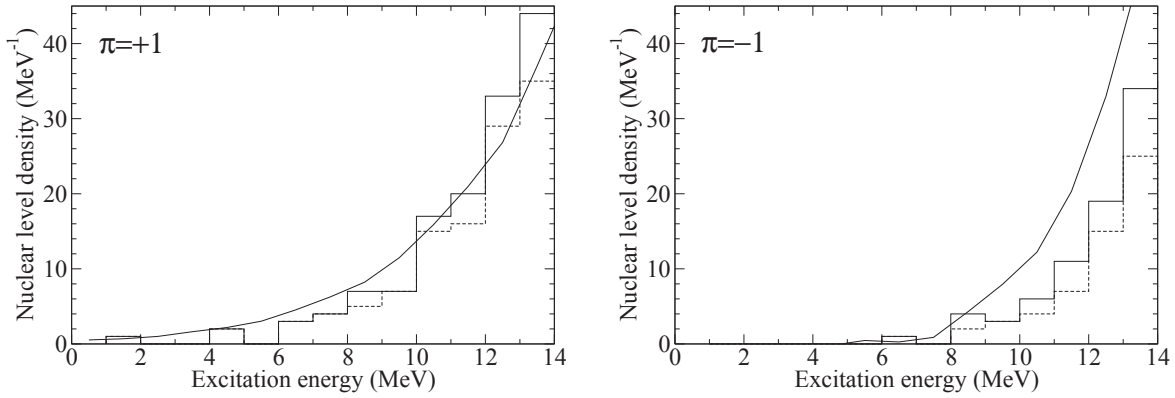


FIGURE 2. ^{28}Si , all J , both parities. Comparison of nuclear level densities from experiment (stair curves) and calculated with the moments method (straight line). Calculation were performed in a s - p - sd - pf model space, up to $1\hbar\omega$ excitation were included, with WBT effective interaction [17].

truncation. Summarizing the results from Figs. 1 and 2 we can conclude that the moments method is able to provide a reasonably good description of the nuclear level density, at least for not very high excitation energy.

The natural next step in development of theory should be an attempt, in application to many nuclei, to extract the global empirical characteristics, such as temperature, entropy, parameters of phenomenological fits, spin cutoff, and so on in order to bridge the gap between the shell-model theory and convenient statistical descriptions traditionally used by experimentalists.

The standard statistical approaches to NLD were started long ago [11-16]. In such approaches the nuclear levels are treated as the excited states of a Fermi-gas system characterized by excitation energy E corresponding to temperature T . In a statistical consideration, the NLD at given energy is exponentially proportional to the entropy of the system, $\rho \sim \exp(S)$. The more accurate expression for the Fermi-gas NLD can be presented as

$$\rho(E, M) = \frac{\sqrt{\pi}}{12a^{1/4}E^{5/4}} \frac{1}{\sqrt{2\pi\sigma^2}} \exp\left(2\sqrt{aE} - \frac{M^2}{2\sigma^2}\right), \quad (5)$$

where E is the excitation energy, M is the nuclear spin projection, σ is the spin cut-off parameter which is generally related to an effective moment of inertia and temperature, and a is the single-particle level density parameter defined at low energies from $E \approx aT^2$.

The Fermi-gas model formula (5) is quite attractive due to its simplicity and minimalistic computational demands as compared to the shell-model or other microscopic approaches, such as the HFB combinatorial method [18, 19, 20]. In general, one can hope that, with excitation energy growing, we deal with very complicated ‘‘chaotic’’ wave functions, while the regular statistical features related to the mean field and Fermi-statistics will survive. On the other hand, treating a real nucleus as a low-temperature Fermi-gas is a rough approximation, the distribution over spin projections and parity is usually introduced phenomenologically, and the density parameters such as a and σ have to be fit to individual nuclei. In this work we compare the real NLD (calculated with the moments method in a realistic model space) with the Fermi-gas description. From such a comparison we hope to be able to conclude how good the traditional Fermi-gas model is for a description of realistic nuclear systems and try to find the optimal Fermi-gas parameters and their evolution along the nuclear chart.

First we discuss the spin cut-off parameter σ . Following the standard ideas of random angular momentum coupling, we can plot $\ln[\rho(E, M)]$ as a function of M^2

$$\ln[\rho(E, M)] = \ln[\rho(E, 0)] - \frac{1}{2\sigma^2}M^2, \quad (6)$$

where

$$\ln(\rho(E, 0)) = 2\sqrt{aE} - \frac{5}{4} \ln[E] + \text{constant}. \quad (7)$$

Fig. 3 presents the corresponding plots for ^{28}Si , ^{52}Fe , ^{44}Ca , and ^{64}Cr isotopes. Different colors refer to different excitation energies: 5 MeV (black), 10 MeV (red), 15 MeV (green), 20 MeV (blue), and 25 MeV (brown). Dots

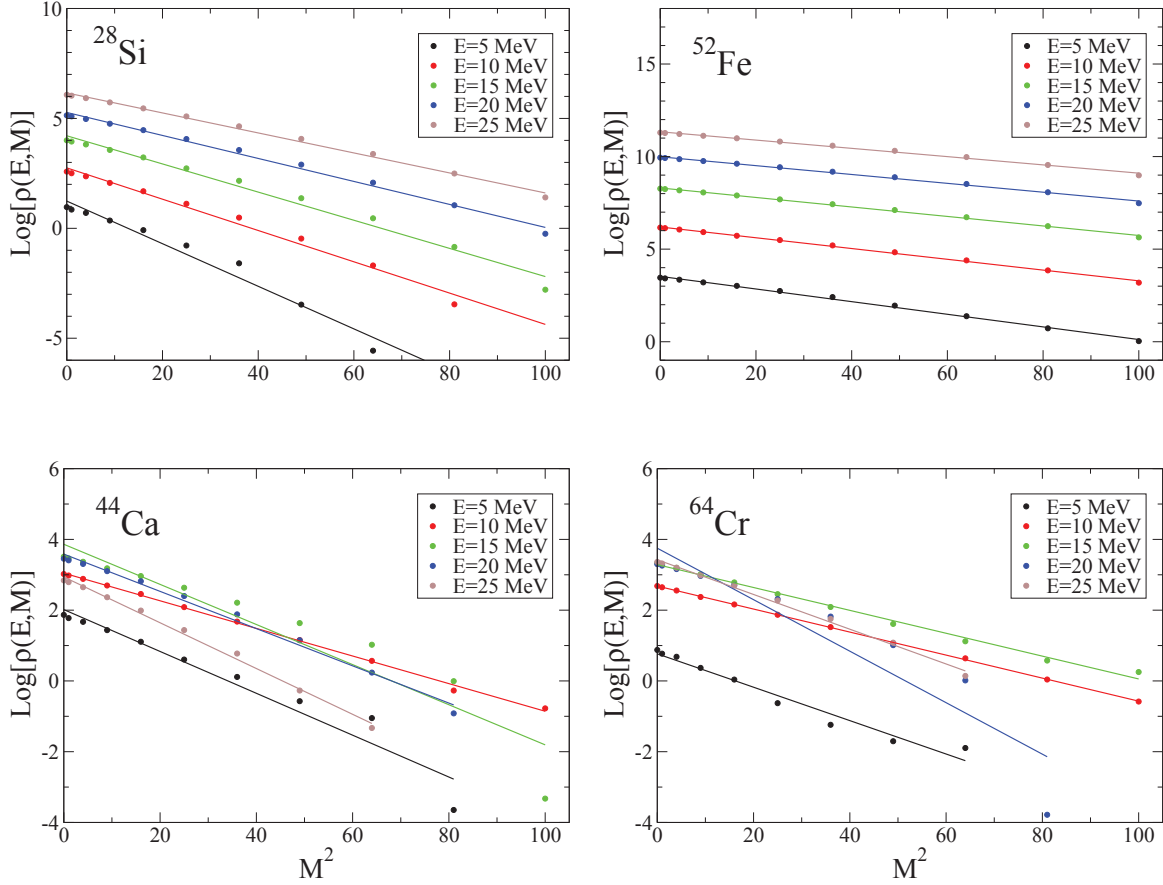


FIGURE 3. Logarithm of level density, $\ln[\rho(E, M)]$, versus M^2 , see Eq. (6), calculated for ^{28}Si , ^{52}Fe , ^{44}Ca , and ^{64}Cr . Different colors present different excitation energies: 5 MeV (black), 10 MeV (red), 15 MeV (green), 20 MeV (blue), and 25 MeV (brown). Dots correspond to the moments-method calculations, the solid lines are linear interpolations, see the text.

correspond to the moments-method densities. The solid lines show the best linear interpolations, for each line we can determine the slope that can be related to the spin cut-off parameter and the constant (at $M = 0$) that corresponds to $\ln[\rho(E, 0)]$, see Eq. (6). From Fig. 3 we see that for ^{28}Si and ^{52}Fe isotopes $\ln[\rho]$ is linearly proportional to M^2 with a good accuracy; the slope and the constant values depend very smoothly on the excitation energy. But for the isotopes ^{44}Ca and ^{64}Cr the situation is different: the linear approximation is not good and the energy dependence is irregular. It turns out that ^{44}Ca and ^{64}Cr belong to a group of nuclei where NLD cannot be well described with the Fermi-gas formula (5). In all nuclei of this type, the isospin-0 channel of interaction is suppressed and only the isospin-1 channel works. Indeed, the ^{44}Ca nucleus has only four valence neutrons in the pf model space, so that only the isospin-1 part of the two-body effective interaction V from Eq. (1) works. The same happens to ^{64}Cr , in the pf model space all neutron states ($N = 40$) are occupied, the active degrees of freedom correspond to only four protons which again switches off the isospin-0 part of the interaction. For the future interpolation procedures we will keep this note in mind.

Assuming that the linear approximation (6) approximately works (at least for a set of nuclei) we can try to extract the spin cut-off parameter σ . For σ it is natural to suggest the following energy (temperature) dependence, since $\sigma^2 \sim T \sim \sqrt{E}$:

$$\sigma^2 = \alpha\sqrt{E}(1 + \beta E), \quad (8)$$

where α and β are the fitting parameters. To fit these parameters we selected the energy interval from 5 to 25 MeV to be used for interpolation. The excitation energy should be sufficiently high to justify the statistical methods and sufficiently low to be able to use a restricted model space. Fig. 4 presents the results of such an interpolation according to Eq. (8). On the left panel one can see α and β parameters fitted for isotopes of calcium (red dots), scandium (green

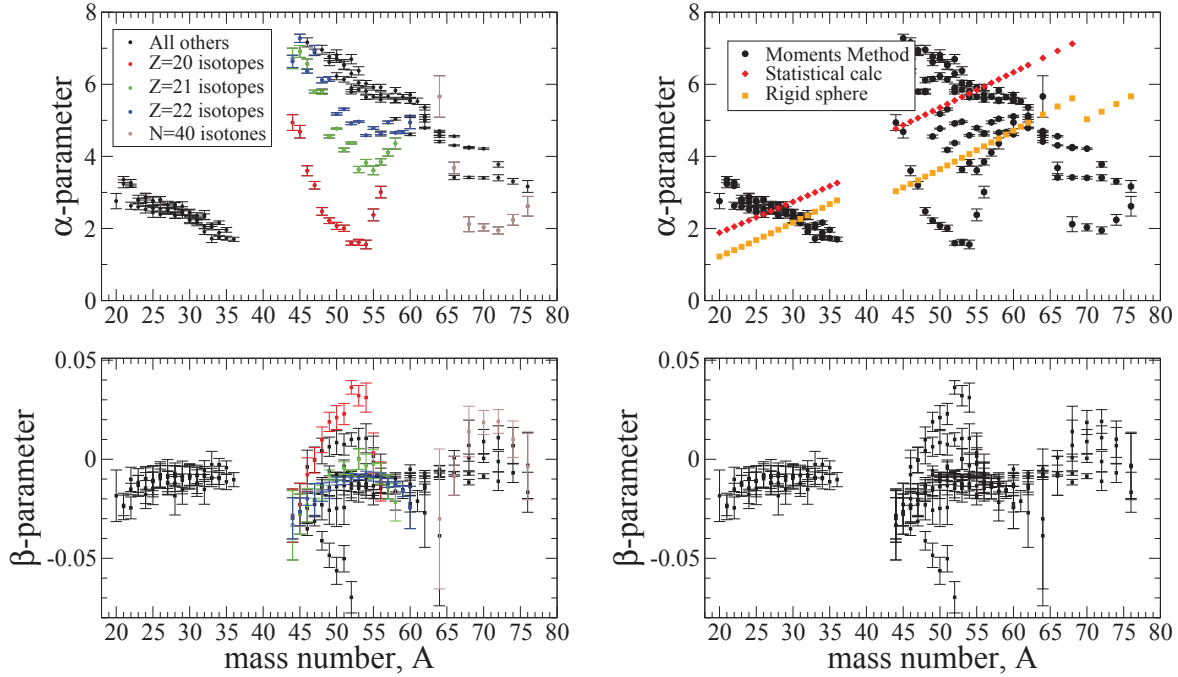


FIGURE 4. Interpolation of the spin cut-off parameter σ^2 , see Eq. (8). Parameters α and β are shown for different *sd* and *pf* nuclei. Left panel: different colors present different isotopes or isotones. Right panel: moments-method calculation with interpolation (black circles), statistical calculation (orange diamonds), rigid sphere approximation (yellow squares).

dots), titanium (blue dots), and $N = 40$ isotones (brown dots). The black dots present all the other *sd* and *pf* nuclei. The isotopes with the zero ground state isospin (coloured dots) expose a clear shell-structure behavior and are slightly off line. The right panel of Fig. 4 shows the comparison of the α parameter from the moments-method calculations (all black dots) with statistical calculations ($\sigma^2 \sim gT\langle M^2 \rangle$, orange diamonds) and with the rigid sphere moment-of-inertia approximation ($\sigma^2 \sim TM_p A^{5/3}$, yellow squares). We can conclude that the shell-model results are in a remarkable agreement with both statistical and moment-of-inertia based calculations. It is interesting to note that, inside a separate shell (the left island for the *sd* shell and the right island for the *pf* shell), σ^2 goes down opposite to the statistical and rigid sphere predictions which would lead to a growth with mass number A as $\sigma^2 \sim A^{5/3}$.

Fig. 5 presents the similar interpolation results for the level density parameter a , see Eq. (7), that is typically considered as coming from the single-particle level density at the Fermi surface. The colouring scheme on the left panel coincide with the corresponding scheme from Fig. 4. Again we can clearly see the shell-structure effects and the isospin-suppressed nuclei are slightly off the common picture. The right panel shows the comparison between the moments-method calculations of this parameter (black circles), the fit from experimental data on neutron resonances (Ref. [21], orange diamonds), and the fit using experimental low-lying levels ([22], yellow squares). We see that the level density parameter a calculated with the moments method is noticeably lower than the corresponding value extracted from fitting to experimental data. It could mean that the moments method NLD grow up with the excitation energy not as fast as the experimental densities. The situation is not clear and demands additional investigation, we leave it for the near future. A natural explanation of the observed discrepancy is that the moments-method NLD (and the shell-model as such) is losing some levels at higher excitation energies due to the restricted model space.

We have presented the first results of studying the nuclear level density by its (practically exact) calculation in the framework of the shell model with mean-field single-particle orbitals and effective residual interaction that describes rather well the low-lying spectroscopic data. The moments method essentially exactly reproduces the level density for given exact quantum numbers as a function of excitation energy avoiding the diagonalization of prohibitively large Hamiltonian matrices. The justification of the method is in complexity of the many-body wave functions that brings the dynamics into the stage of thermalization and quantum chaos. The validity of the approach is intrinsically limited by energies where the contribution from the orbital space excluded from the shell model becomes important. By our

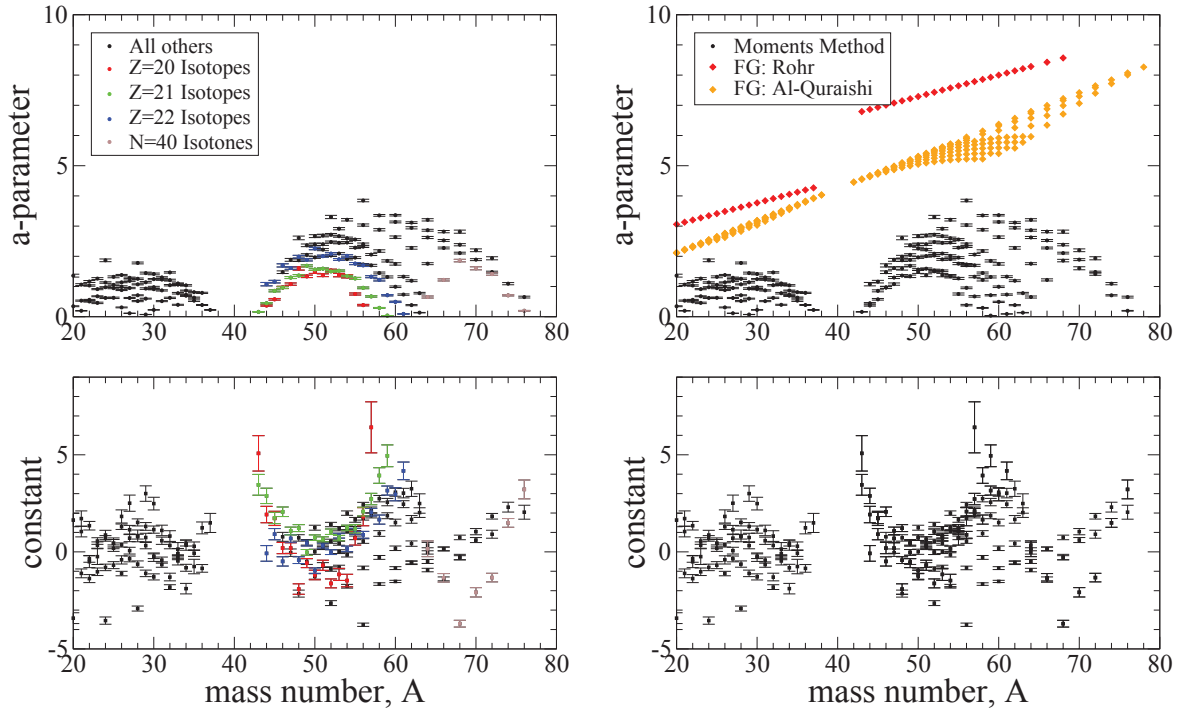


FIGURE 5. Interpolation of the single-particle level density parameter a , see Eq. (7). Left panel: different colors present different isotopes or isotones. Right panel: moments-method calculation with interpolation (black circles), fit using the experimental data on neutron resonances (Ref. [21], orange diamonds), and fit using experimental low lying levels ([22], yellow squares).

estimates, it can be used rather safely at least up to 15-20 MeV excitation energy. The limitation from above comes also from the continuum that converts mean-field levels into the resonances, so that the concept of the discrete level density becomes less definite when the resonances start to overlap.

We just started the comparison of the results of the moments method with standard phenomenological expressions used by generations of physicists. There are still many open questions which we hope to address in the future. An interesting physical problem to be discussed elsewhere is the understanding of the role played by various components of the residual interaction in forming the level density.

ACKNOWLEDGMENTS

Support from the NUCLEI SciDAC Collaboration under U.S. Department of Energy Grant No. DE-SC0008529 is acknowledged. V.Z. and M.H. also acknowledge U.S. NSF Grants No. PHY-1404442 and PHY-1068217.

REFERENCES

1. S. S. M. Wong, *Nuclear Statistical Spectroscopy*, Oxford, University Press, 1986.
2. V. K. B. Kota and R. U. Haq, *Spectral Distributions in Nuclei and Statistical Spectroscopy*, World Scientific, Singapore, 2010.
3. T. A. Brody, J. Flores, J. B. French, P. A. Mello, A. Pandey, and S. S. M. Wong, *Rev. Mod. Phys.* **53**, 385 (1981).
4. R. A. Sen'kov, M. Horoi, and V. Zelevinsky, *Phys. Lett. B* **702**, 413 (2011).
5. R. A. Sen'kov, M. Horoi, and V. Zelevinsky, *Comp. Phys. Comm.* **184**, 215 (2013).
6. NuShellX@MSU, B.A. Brown, W.D.M. Rae, E. McDonald, and M. Horoi, <http://www.nsc1.msu.edu/~brown/resources/resources.html>
7. M. Horoi, A. Volya, and V. Zelevinsky, *Phys. Rev. Lett.* **82**, 2064 (1999).
8. M. Horoi, B. A. Brown, and V. Zelevinsky, *Phys. Rev. C* **65**, 027303 (2002).
9. B. A. Brown and B. H. Wildenthal, *Annu. Rev. Nucl. Part. Sci.* **38**, 29 (1988).
10. V. Zelevinsky, B. A. Brown, N. Frazier, and M. Horoi *Phys. Rep.* **276**, 85 (1996).

11. Ya. I. Frenkel, *Sov. Phys.* **9**, 533 (1936).
12. H. Bethe, *Phys. Rev.* **50**, 332 (1936).
13. H. Bethe, *Rev. Mod. Phys.* **9**, 69 (1937).
14. L. D. Landau, *J. Exp. Theor. Phys.* **7**, 819 (1937).
15. T. Ericson, *Adv. Phys.* **9**, 425 (1960).
16. A. Gilbert and A. G. W. Cameron, *Can. J. Phys.* **43**, 1446 (1965).
17. E. K. Warburton and B. A. Brown, *Phys. Rev. C* **46**, 923 (1992).
18. S. Goriely, S. Hilaire, and A. J. Koning, *Phys. Rev. C* **78**, 064307 (2008).
19. S. Goriely, S. Hilaire, A. J. Koning, M. Sin, and R. Capote, *Phys. Rev. C* **79**, 024612 (2009).
20. <http://www.astro.ulb.ac.be/pmwiki/Bruslib/Level>
21. G. Rohr, *Z. Phys. A* **318**, 299 (1984).
22. S. I. Al-Quraishi, S. M. Grimes, T. N. Massey, and D. A. Resler, *Phys. Rev. C* **63**, 065803 (2001).